Angewandte Chemie
Eine Zeitschrift der Gesellschaft Deutscher Chemiker

Supporting Information

69451 Weinheim, Germany

Coexistence of Distinct Single-Ion and Exchange-Based Mechanisms for Blocking of Magnetization in a $Co^{II}_2Dy^{III}_2$ Single-Molecule Magnet**

Kartik Chandra Mondal, Alexander Sundt, Yanhua Lan, George E. Kostakis, Oliver Waldmann, Liviu Ungur, Liviu F. Chibotaru,* Christopher E. Anson, and Annie K. Powell**

anie_201201478_sm_miscellaneous_information.pdf

Preparation of $[Co_2Dy_2(L)_4(NO_3)_2(THF)_2]\cdot 4THF$ (1): The mixture of $Dy(NO_3)_3\cdot 6H_2O$ (0.1 mmol, 45 mg), $Co(NO_3)_2\cdot 6H_2O$ (0.1 mmol, 29 mg) and H_2L (0.2 mmol, 48.6 mg) was stirred in 20 mL of methanol for 1 min in the presence of Et_3N (0.42 mmol, 42 mg). The red color solution was left undisturbed and after 30 min microcrystalline material was precipitated out which was dissolved in 15 mL THF. The slow evaporation from air produced red color block shaped crystals of **1** in 75% yield. Anal. Calc. (%) for $C_{60}H_{62}Dy_2Co_2N_6O_{24}$ corresponding to replacement of some THF by H_2O leading to $[Co_2Dy_2(L)_4(NO_3)_2(THF)(H_2O)]\cdot 4H_2O$ (found): C 42.54 (42.46), N 4.96 (4.95), H 3.68 (3.70). IR (KBr, cm^{-1}): 3414(b), 3057(w), 2942(m), 2835(m), 1606(s), 1586(s), 1546(m), 1517(s), 1481(s), 1459(s), 1439(s), 1386(s), 1331(m), 1290(m), 1255(m), 1225(s), 1182(w), 1108(w), 1075(w), 1019(w), 966(m), 822(w), 737(s), 642(w), 588(w), 520(w).

Preparation of $[Co_2Y_2(L)_4(NO_3)_2(THF)_2]\cdot 4THF$ (2): The same synthetic procedure for **1** was followed, but using $Y(NO_3)_3.6H_2O$ in place of $Dy(NO_3)_3\cdot 6H_2O$, giving **2** in 65% yield. The IR spectrum is essentially identical to that of **1**. Anal. Calc. (%) for $C_{60}H_{62}Y_2Co_2N_6O_{24}$ corresponding to replacement of some THF by H_2O leading to $[Co_2Y_2(L)_4(NO_3)_2(THF)(H_2O)]\cdot 4H_2O$ (found): C 46.58 (46.53), N 5.43 (5.45), H 4.04 (4.00).

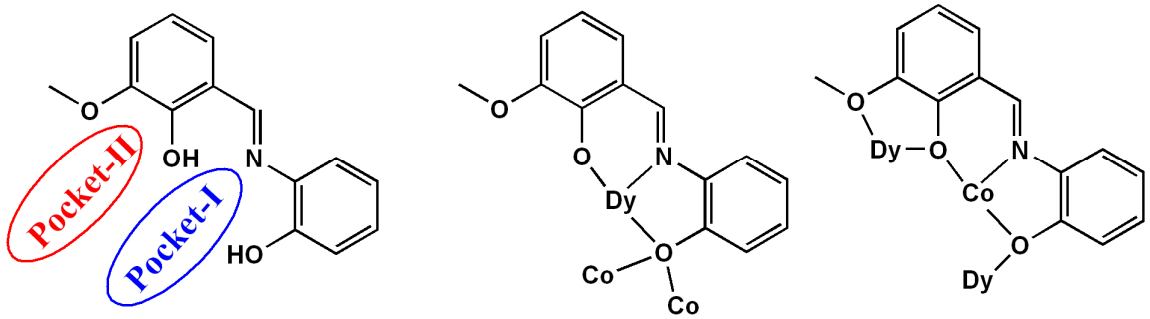

Figure S1. Structure of ligand (H_2L) with two types of pocket (I and II) (left). The observed bridging modes of dianionic ligand (L^{2-}) in complex **1** (middle and right).

Table S1. Crystallographic data of complexes **1** and **2**.

Compound	**1**	**2**
Formula	$C_{80}H_{92}Co_2Dy_2N_6O_{24}$	$C_{80}H_{92}Co_2N_6O_{24}Y_2$
Mr [g mol^{-1}]	1964.46	1817.28
Crystal size [mm]	0.27×0.22×0.18	0.25×0.24×0.11
colour	Red	Red
Crystal System	Triclinic	Triclinic
Space Group	*P*-1	*P*-1
T [K]	150(2)	180(2)
a [Å]	11.7308 (9)	11.7437(12)
b [Å]	13.2206 (11)	13.2227(13)
c [Å]	14.9021 (12)	14.9685(14)
a [°]	109.024 (6)	109.568(7)
ß [°]	93.391 (6)	93.149(8)
? [°]	113.742 (6)	113.694(7)
V [Å^3]	1951.0 (3)	1956.5(3)
?	1	1
?$_{calc}$ [g cm^{-3}]	1.672	1.542
µ(Mo-Ka) [mm^{-1}]	2.393	1.968
F(000)	992	938
Reflns collected	16703	13449
Unique data	9316	8261
R_{int}	0.0256	0.0209
Data with *I* > 2s (I)	8192	7037
parameters/restraints	510 / 68	510 / 68
S on *F* ^{2}	1.00	1.015
R_1 [*I* > 2s (I)]	0.0411	0.0378
wR_2 (all data)	0.1060	0.1006
Largest diff. peak/hole [e Å^{-3}]	+0.86 / -2.46	+0.74 / -0.55
CCDC No.	853440	853441

Table S2. Selected bond lengths (Å) and bond angles (°) within the coordination cluster in **1**.

Dy1—O1	2.155 (3)	Dy1—O7	2.441 (3)	Dy1—N3	2.892 (3)
Dy1—O4	2.306 (2)	Dy1—N1	2.454 (3)	Dy1—O5	2.518 (3)
Dy1—O6^{i}	2.343 (3)	Dy1—O8	2.480 (3)	Dy1—O3	2.390 (3)
Co1—O6	2.036 (3)	Co1—O3^{i}	2.261 (3)	Co1—O10	2.197 (3)
Co1—O4	2.038 (3)	Co1—O3	2.077 (2)	Co1—N2	2.062 (3)
Dy1—Co1	3.4962 (6)	Co1—Dy1^{i}	3.4886 (6)	O3–Co1Co1´Dy1	1.069
Co1—O3—Dy1	102.77 (10)	Co1—O4—Dy1	107.03 (10)	Co1—O6—Dy1^{i}	105.41 (10)
C28—O6—Dy1^{i}	121.1 (2)	Co1^{i}—O3—Dy1	97.15 (9)		

Symmetry code: (i) - *x*+1, - *y*+1, - *z*+1**.**

Description of structure

Complex **1** crystallizes in the triclinic space group *P*-1 with Z = 1. Within the core of the centrosymmetric complex, the metal ions are linked by four $(L)^{2-}$ ligands into the familiar butterfly or defect-dicubane topology. (Figure 1). One of the two crystallographically independent ligands chelates Dy(1) through its imine nitrogen and the two phenolate oxygens O(1) and O(3) (corresponding to Pocket I, see Fig S1). Co(1) and Co(1') are linked via a μ_3-OR-bridge from the phenolate O(3) which also connects to Dy(1) to form a Co_2Dy triangle. The other ligand chelates Co(1) via Pocket I as well as the O(4) and O(5) donors of Pocket II which also coordinate Dy(1) with the aminophenolate O(6) bridging to Dy(1'). The coordination spheres of the metal ions are completed though the ligand and its inversion equivalent providing μ-OR bridges along the four outer edges of the Co_2Dy_2 rhombus the coordination spheres of the Dy completed by nitrate ligands chelating the heptacoordinated Dy ions with the final coordination site on the hexacoordianted Co ions provided by the O(10) oxygen of a THF ligand.

Co(1) has a slightly distorted octahedral geometry with an O_5N donor set. The O_7N donor set about Dy(1) is close to a pentagonal-bipyramidal geometry with the chelating nitrate on an axial site. (Figure S2). The Co-O/N and Dy-O/N bond distances are in the ranges 2.036-2.261 Å and 2.155-2.518 Å respectively. The angles Co1-O3-Co1´, Co1-O3-Dy1, Co1-O3-Dy1´, Co1-O4-Dy1 and Co1-O6-Dy1´ at the bridging oxygens are 96.91(10), 102.77(10), 97.15(9), 107.03(10) and 105.41(10)°, respectively. Within the crystal structure of **1**, the tetranuclear complexes are surrounded by lattice THF molecules which prevent any intercomplex π-π stacking, (Figure 1). The intermolecular Dy··Dy distances are over 10 Å. Selected bond lengths and angles are given in Table S2.

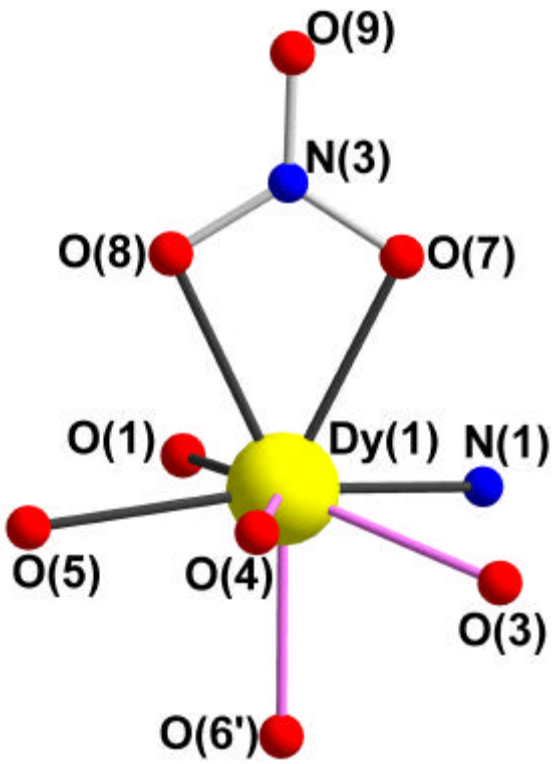

Figure S2. Coordination geometry of Dy(1) in complex **1**.

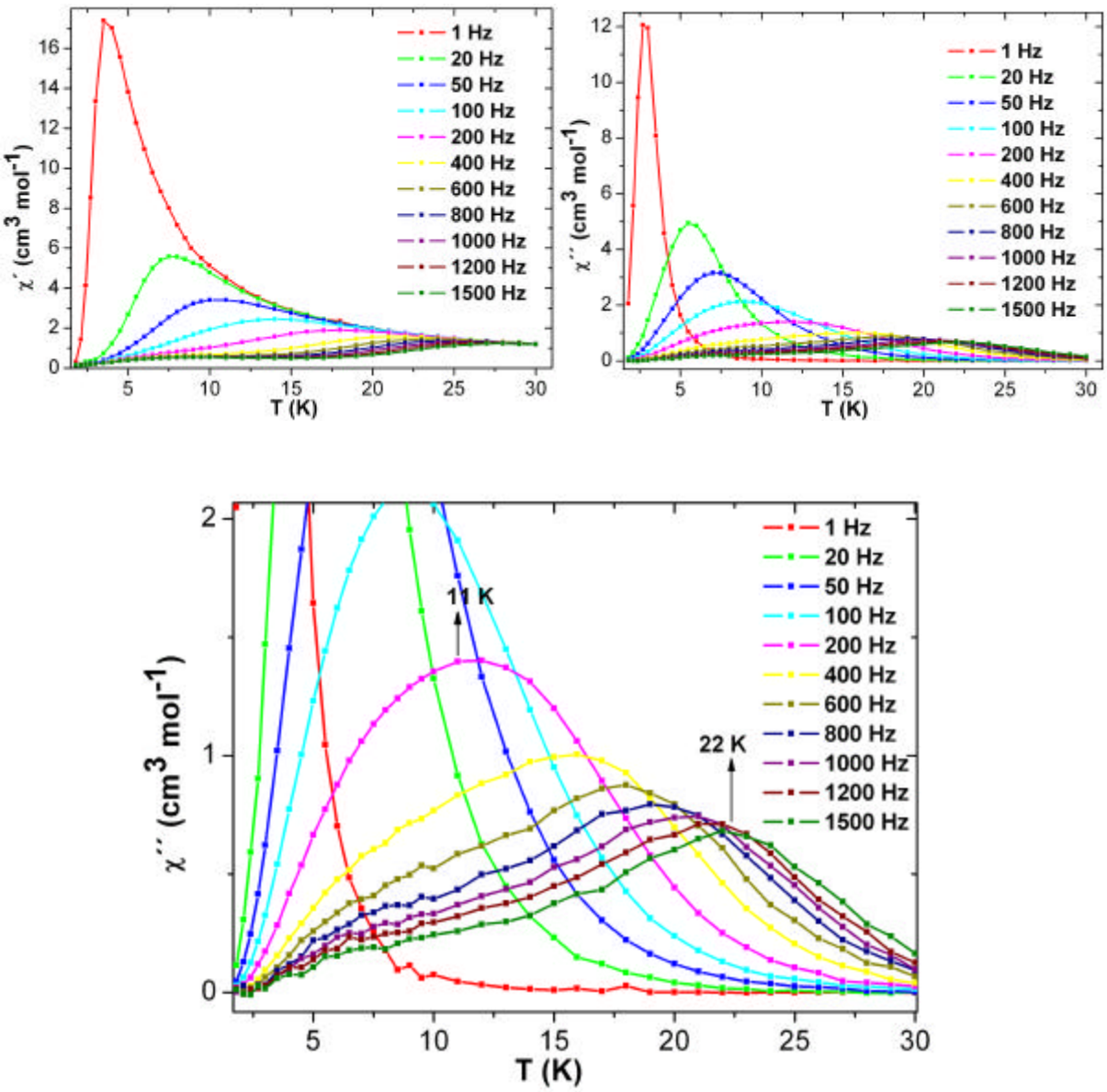

Figure S3. Top: plots of ?´ vs T (left) and ?'' vs T (right) of **1** at indicated frequencies. Down: Zoom-in of plot of ?'' vs T.

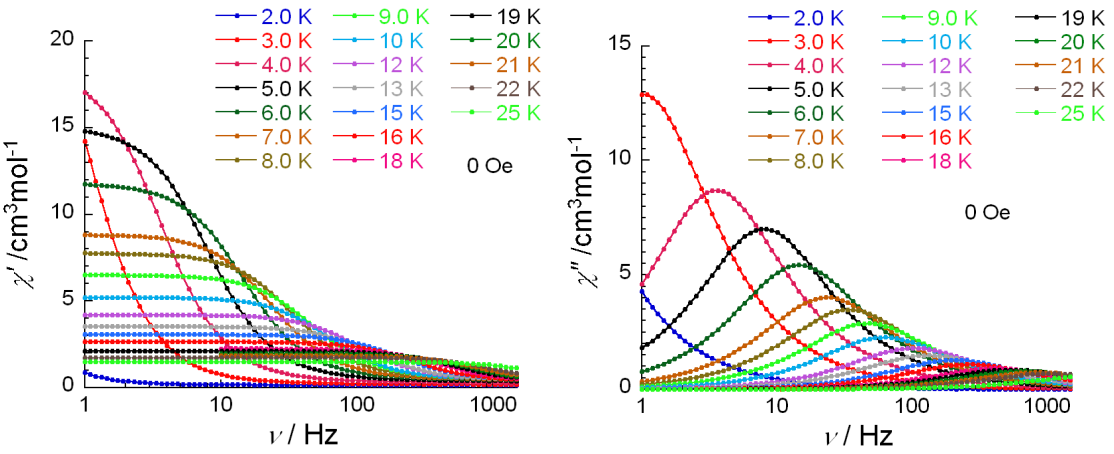

Figure S4. ?´ vs log(v) (left) and ?´´ vs log(v) (right) plots of **1** at indicated temperatures.

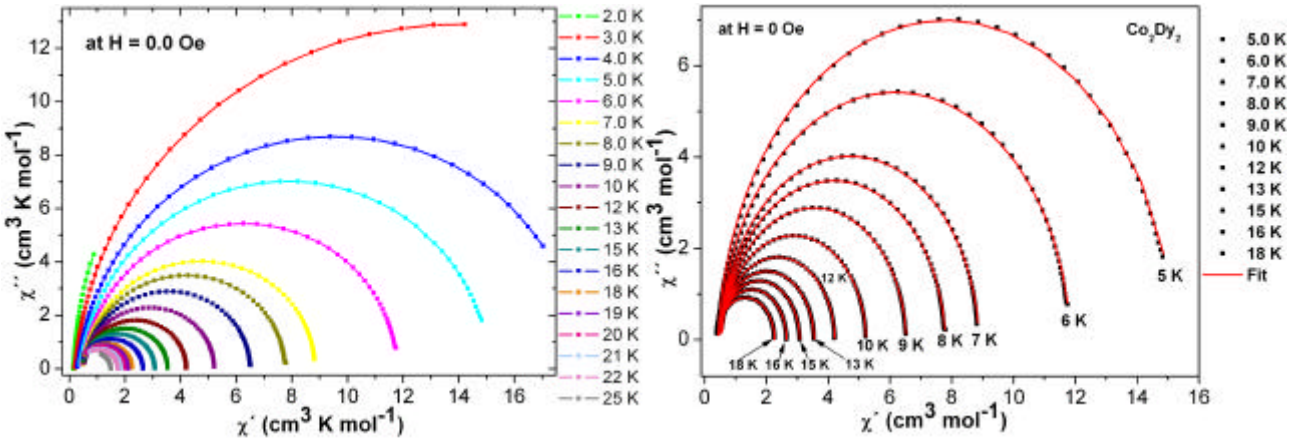

Figure S5. Cole-Cole plots of **1** at indicated temperatures (left). The red solid lines (right) correspond to the fits to the generalized Debye model. See more details in the text.

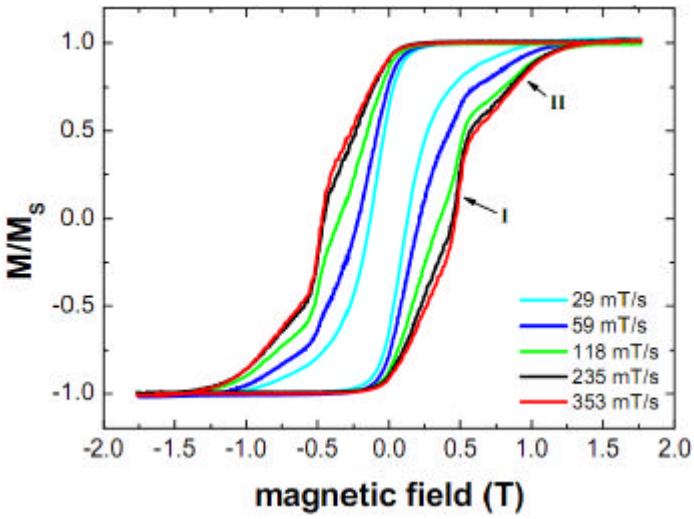

Figure S6. Hysteresis loops of **1** at 1.5 K with different sweeping rates.

Table S3 Analysis of Cole-Cole plot of **Co_2Dy_2** complex.

T (K)	$?_0$ (cm^3/mol)	$?_{inf}$ (cm^3/mol)	a	R^2
3	28.946(107)	0.208(1)	0.0450(1)	---
4	18.857(35)	0.325(5)	0.0401(1)	---
5	15.210(16)	0.431(6)	0.0349(12)	0.99996
6	11.850(10)	0.504(6)	0.0292(13)	0.99996
7	8.878(7)	0.529(5)	0.0246(14)	0.99995
8	7.786(5)	0.5545(48)	0.0242(13)	0.99996
9	6.525 (3)	0.5588(41)	0.0213(12)	0.99996
10	5.226 (26)	0.5351(35)	0.0181(12)	0.99996
12	4.216 (11)	0.5105(30)	0.0160(11)	0.99997
13	3.542(1)	0.480 (3)	0.0139(12)	0.99996
15	3.076(1)	0.4532(22)	0.0120(1)	0.99998
16	2.650(10)	0.4195(37)	0.0092(15)	0.99994
18	2.262(1)	0.4023(54)	0.0081(21)	0.99992
19	2.104(1)	0.4714(45)	0.0071(76)	0.99778
20	1.971(1)	0.3693(110)	0.0061(32)	0.99982
21	1.849(1)	0.4303(128)	0.0052(37)	0.99979

Fragment ab initio calculation of magnetic properties of individual metal centers and estimation of exchange interactions in Dy_2Co_2 complex

Computational Details

The magnetic properties of metal centers in the Dy2Co2 complex have been studied by fragment *ab initio* calculations by using a specially designed routine SINGLE_ANISO[1] interfaced with the MOLCAS package.[2] In this connection, the question arises to cut suitable mononuclear fragments from the molecule, which would not change significantly the energy structure on the magnetic centre. To have a good description of the 3d or 4f ligand-field states within a fragment one needs to take into account the influence of the neighbouring metal ions. To this end the neighbouring Dy^{3+} have been simulated by the closed-shell La^{3+} *ab initio* embedding model potentials (AIMP)[3] and the Co^{2+} have been simulated by Zn^{2+}-AIMP.[3]

The second approximation concerned the coordination sphere. The structures of the calculated fragments are shown in the Figure 2 and 3 below. No geometry optimization on the fragments have been done, all atomic coordinates (except for added hydrogens) being taken from the crystal X-ray analysis. The basis sets used for the calculations were taken from ANO-RCC basis libraries from MOLCAS package.[4]

For the electronic structure, the *ab initio* calculations were performed by means of MOLCAS-7.4 program.[2]

The active space of the complete active space self-consisting field (CASSCF) of calculation of the Dy included the 4f orbitals (CAS (9 in 7) since we are interested in the ligand field states only. The 4f orbitals are known to be localized, which allows us to consider the charge transfer states much higher in energy, thus being not relevant for the magnetism. The active space of the CASSCF calculation of Co^{2+} (CAS9 in 12) included the 7 d-type electrons spanning 10 (3d +3d') orbitals plus a doubly occupied ligand-type orbital and a virtual orbital, for a better description of the hybridization between the 3d-orbitals and ligand-type orbitals.

We have performed several calculations including different number of states in the RASSI-SO calculations for Dy^{3+} fragment. The results are listed below. The number and free ion parentage of states mixed by RASSI are listed together with the fragment description below.

With the obtained spin-orbit multiplets, the powder susceptibility and the g-tensors for the lowest Kramers doublets of isolated fragments were further evaluated using the recently developed *ab initio* methodology.[1] The basis of this approach is to calculate *ab initio* all angular moment matrix elements and then all magnetic moment matrix elements on the relevant spin-orbit multiplets obtained in CASSCF/CASPT2 calculations. These matrix elements are used in a separate routine to calculate:

(i) magnetic properties measured directly in experiment (temperature dependent Van Vleck susceptibility tensor and powder averaged function, field dependent magnetization for different temperatures and directions and the powder magnetization) and

(ii) (ii) parameters of magnetic spin Hamiltonians for different spin-orbit multiplets and groups of spin states, described by the corresponding pseudospin, (*g* tensors, zero-field splitting tensors).

In calculations of magnetic properties, all spin-orbit multiplets on the sites are usually taken into account, in particular, all ligand-field states in the case of transition metal ions. This is important for correct quantitative account of the effects of strong magnetic anisotropy and strong applied magnetic fields. Computationally, this routine (SINGLE_ANISO) was interfaced with MOLCAS-7.4 program.

For the simulation of magnetic properties of polynuclear complexes we used an approach combining the calculated magnetic properties of individual metal fragments (CASSCF /RASSI-SO + SINGLE_ANISO) with the description of anisotropic exchange interaction between metal sites. The exchange model including two structural chain units which have been explicitly taken into account is depicted in the Figure 2. The simulations have been done with a specially designed routine POLY_ANISO[1]. Both programs were interfaced with the SINGLE_ANISO routine treating individual metal fragments.

This *ab initio* based methodology has already been successfully applied for the treatment of the effects of strong magnetic anisotropy in polynuclear transition metal complexes. Thus it allowed to explain the origin of non-magnetic ground state in Dy_3 triangles,[7a] to understand the complex magnetism in mixed-valent $Co^{II}_3Co^{III}_4$ heptanuclear wheel, in particular, the lack of SMM behaviour in this compound,[7b] to explain the unusual magnetism of single-chain magnets.[7c]

References:

1. L. F. Chibotaru, L. Ungur, Programs SINGLE_ANISO and POLY_ANISO, University of Leuven 2006.
2. G. Karlström, R. Lindh, P. -Å. Malmqvist, B. O. Roos, U. Ryde, V. Veryazov, P. -O. Widmark, M. Cossi, B. Schimmelpfennig, P. Neogrady, L. Seijo, *Comp. Mater. Sci.* **2003**, *28*, 222-239.
3. L. Seijo, Z. Barandiarán, in *Computational Chemistry: Reviews of Current Trends* **1999,** *4*, ed. by J. Leszcynski (World Scientific, Singapur), 55-152.
4. B. O. Roos, R. Lindh, P-O. Malmqvist,V. Veryazov V., P. O. Widmark, *J. Phys. Chem. A,* **2004**, *108*, 2851.
5. K. Andersson, B. O. Roos, *Chem. Phys. Lett.* **1992**, *191*, 507-514.
6. B. O. Roos, P-O. Malmqvist, *Phys. Chem. Chem. Phys.* **2004**, *6*, 2919-2927.
7. a) L. Ungur, W. Van den Heuvel, L. F. Chibotaru, *New J. Chem.*, **2009**, *33*, 1224-1230.; b) L. F. Chibotaru, L. Ungur, Ch. Aronica, H. Elmoll, G. Pilet, D. Luneau, *J. Am. Chem. Soc.* **2008**, *130* (37), 12445-12455.; c) D. Visinescu, A. M. Madalan, M. Andruh, C. Duhayon, J.-P. Sutter, L. Ungur, W. Van den Heuvel, L. F. Chibotaru *Chem. Eur. J.* **2009**, *15*, 11808 – 11814.

CASSCF calculations of metal fragments of Dy_2Co_2 complex

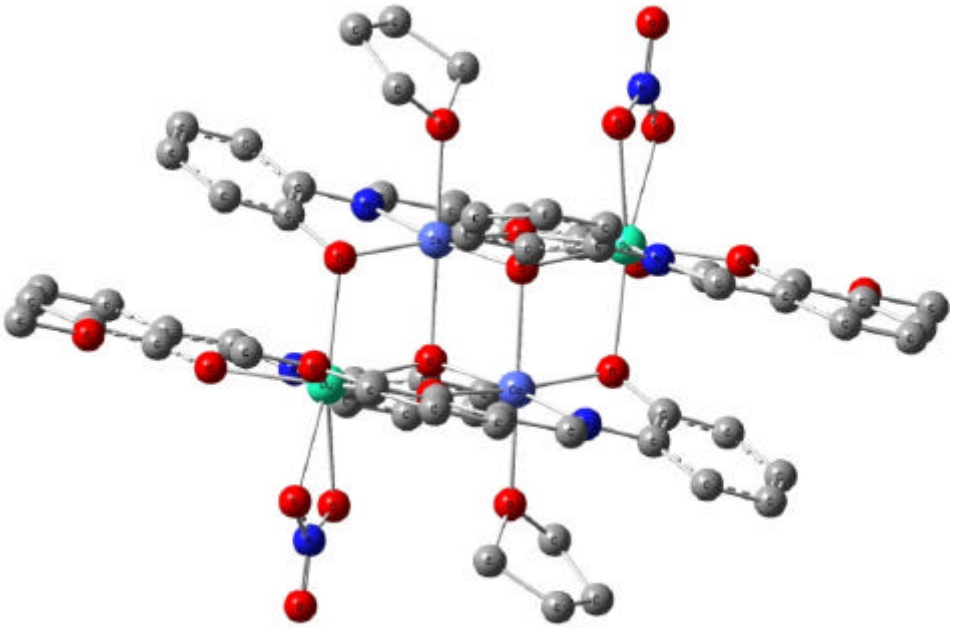

Figure S7. The structure of the Dy_2Co_2 complex.

Fragment Dy^{III}

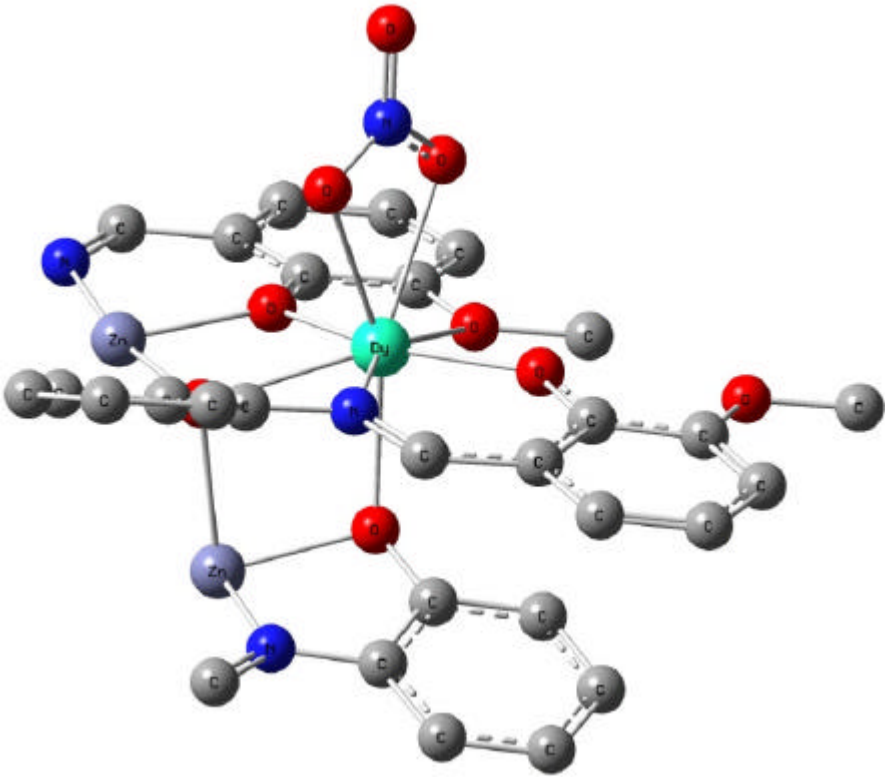

Figure S8. The structure of the calculated Dy^{3+} fragment.

Basis Sets
ANO-RCC [7s6p4d3f1g] – for Dy^{3+}.
ANO-RCC [3s2p1d] – for close O and N.
ANO-RCC [3s2p] – for C and distant O and N.
ANO-RCC [2s] – for H.
ECP---Zn.ECP.Lopez-Moraza.0s.0s.0e-AIMP-KZnF3. – for Co^{2+}.

Active space:
CAS(9 in 7).

Calculated roots:
In the best calculation all the states coming from the following multiplets have been taken into account in the spin-orbit interaction (RASSI): ^{6}H, ^{6}F, ^{6}P (all sextets), ^{4}I, ^{4}F, ^{4}M, ^{4}G, ^{4}L, ^{4}D, ^{4}H, ^{4}P, ^{4}G, ^{4}F, ^{4}I (128 out of 224 quartets), ^{2}L, ^{2}K, ^{2}P, ^{2}N, ^{2}F, ^{2}M, ^{2}H, ^{2}D, ^{2}G, ^{2}O (130 out of 490 doublets).

Table S4: Lowest calculated terms and Kramers doublets on Dy^{3+} fragment.

	Spin Multiplicity	CASSCF (cm^{-1})	Kramers doublets (cm^{-1})		
			^{6}H	^{6}H, ^{6}F, ^{6}P	279 states
1	6	0.000	0.000	0.000	0.000
2	6	11.281	193.564	193.576	192.638
3	6	281.869	313.881	312.376	307.743
4	6	330.145	393.415	392.586	386.288
5	6	387.486	438.773	437.877	430.910
6	6	413.376	519.410	518.482	509.070
7	6	518.543	576.541	575.646	565.837
8	6	542.229	642.249	640.837	627.906
9	6	671.315	3102.999	3103.322	3653.864
10	6	751.243	3256.363	3256.524	3804.767
11	6	785.353	3333.170	3333.056	3881.154
12	6	7728.605	3385.999	3385.609	3933.577
13	6	7799.819	3432.672	3432.480	3980.295
14	6	7813.647	3464.914	3464.900	4012.233
15	6	7906.440	3539.671	3539.331	4086.079
16	6	7945.694	5744.296	5744.407	6243.305
17	6	8002.667	5842.057	5841.794	6334.012
18	6	8030.167	5924.540	5924.219	6411.878
19	6	34867.808	5973.284	5973.261	6468.812
20	6	35223.819	6020.737	6020.344	6517.712
21	6	35303.637	6096.191	6095.678	6579.388
1	4	24951.030	7951.920	7949.637	8219.004
2	4	24953.333	8039.076	8036.651	8303.995
3	4	25074.850	8122.232	8121.014	8386.573
4	4	25078.212	8183.858	8182.427	8447.922
5	4	25106.994	8259.312	8255.963	8520.029
…	…	…	9739.724	9707.030	9753.612
1	2	37439.172	9849.681	9757.954	9858.146
2	2	37442.084	9946.478	9778.974	9951.452
3	2	37488.990	10039.974	9805.148	10042.196
4	2	37495.747	11126.543	9819.109	10193.762
5	2	37522.444	11320.920	9860.065	10219.732
…	…	…	…	…	…

Table S5: The g-tensor of the ground Kramers doublet of Dy^{3+}.

	Spin-Orbit energy (cm^{-1})	g tensor of the ground KD		
		^{6}H	^{6}H, ^{6}F, ^{6}P	279 states
1	0.000	g_x= 0.0056 g_y= 0.0088 g_z= 19.6286	g_x= 0.0056 g_y= 0.0096 g_z= 19.6311	g_x=0.0052 g_y=0.0084 g_z=19.5325

Fragment Co^{II}

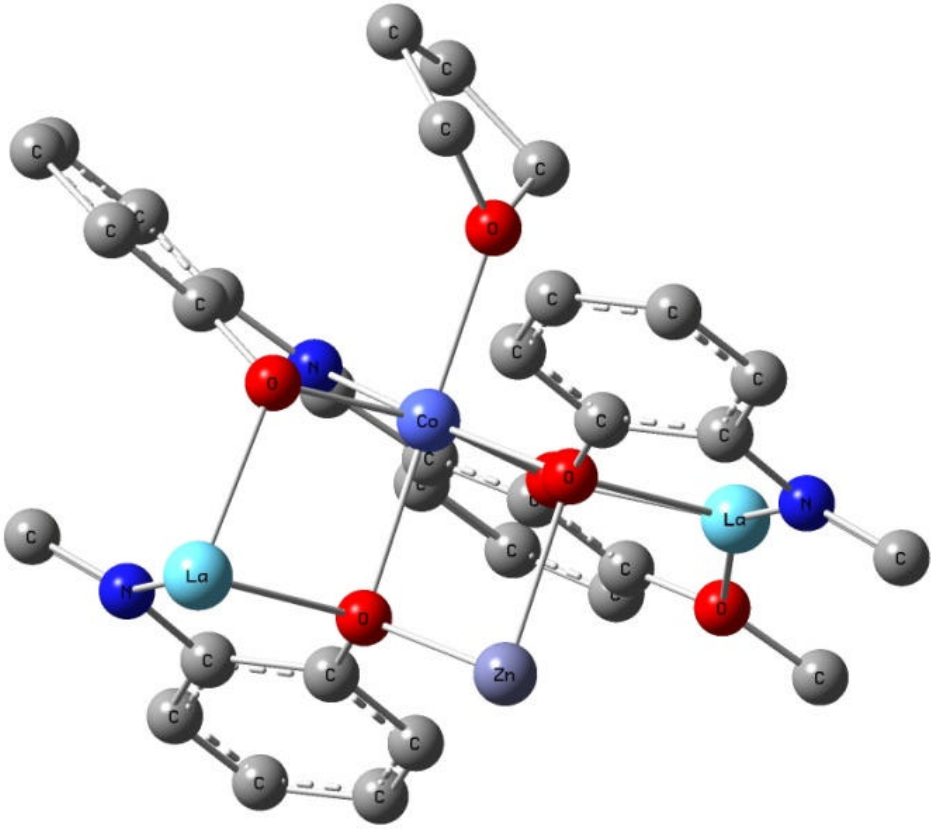

Figure S9. The structure of the calculated Co^{2+} fragment.

Basis Sets
ANO-RCC [8s7p5d4f2g1h] – for Gd^{3+}.
ANO-RCC [3s2p1d] – for O and N.
ANO-S [3s2p1d] – for C.
ANO-S [2s1p] – for H.
ECP---La.ECP.deGraaf.0s.0s.0e-La(LaMnO3). – for Dy^{3+}.
ECP---Zn.ECP.Lopez-Moraza.0s.0s.0e-AIMP-KZnF3. – for Co^{2+}.

Active space:
CAS(9 in 12).

Calculated roots:
All the states coming from the following multiplets have been taken into account in the spin-orbit interaction (RASSI): ^{4}F, 4P (all quartets), ^{2}D, ^{2}N, ^{2}H, ^{2}F, 2^{2}D, ^{2}P (all doublets).

Table S6: Lowest calculated terms and Kramers doublets on Dy^{3+} fragment.

	Spin Multiplicity	CASSCF (cm^{-1})	Kramers doublets (cm^{-1})
1	4	0.000	0.000
2	4	1014.840	109.077
3	4	1368.876	1045.527
4	4	5633.487	1276.263
5	4	8500.907	1624.054
6	4	9093.864	1750.800
7	4	16076.811	5848.236
8	4	21958.306	5925.972
9	4	22847.693	8672.860
10	4	26144.920	8720.651
1	2	11994.215	9283.366
2	2	15689.673	9384.054
3	2	17862.131	12212.782
4	2	18479.609	15892.430
5	2	19697.015	16322.917
…	…	…	…

Table S7: The g-tensor of the ground Kramers doublet of Dy^{3+}.

	Spin-Orbit energy (cm^{-1})	g tensor of the ground KD
1	0.000	g_x= 1.8934 g_y= 3.2383 g_z= 6.7429

Simulations of magnetism and evaluation of exchange interactions between magnetic centers in Dy_2Co_2

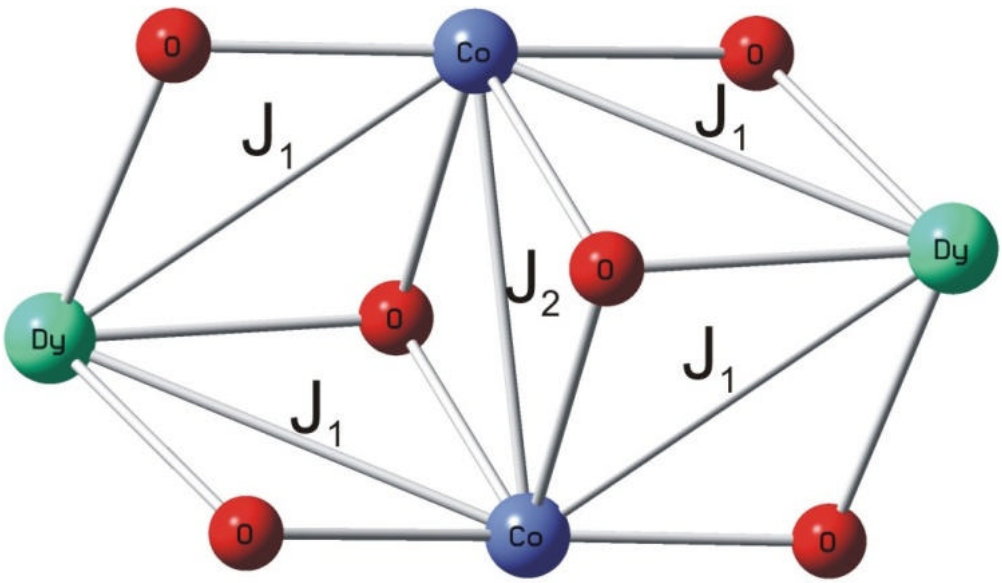

Figure S10. Exchange interactions considered in describing the magnetism of the Dy_2Co_2.

The employed model of the exchange interactions within the Lines approximation (computationally done with the POLY_ANISO software [1]) is given by the following isotropic Hamiltonian:

$$H = -J_{Dy-Co}\left(S_{Dy1}S_{Co1} + S_{Dy1}S_{Co2} + S_{Dy2}S_{Co1} + S_{Dy2}S_{Co2}\right) - J_{Co-Co}S_{Co1}S_{Co2} \quad , \qquad (1)$$

where *S* is the spin of the corresponding center. The best agreement between the calculated and measured magnetism (Figure 2), using the above model Hamiltonian is achieved for: $J_{Dy\text{-}Co}$ = 1.6 cm^{-1} and $J_{Co\text{-}Co}$ = 2.0 cm^{-1}. Due to the strong axiality of the ground Kramers doublet of Dy ions (Table 1) the Lines model (1), when projected onto the ground Kramers doublets of cobalt and dysprosium ions in **1** becomes close to an Ising exchange Hamiltonian.

These parameters were used in the calculation of the temperature dependence of magnetic susceptibility and high-field magnetization at 2K, 3K and 5K.

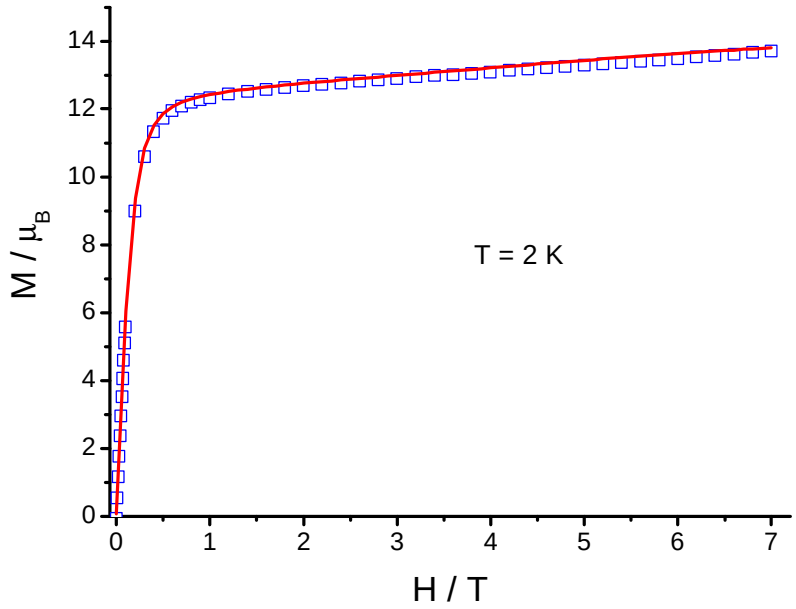

Figure S11. A comparison between experimental (square) and calculated (line) powder molar magnetization of the Dy_2Co_2 complex at 2K.

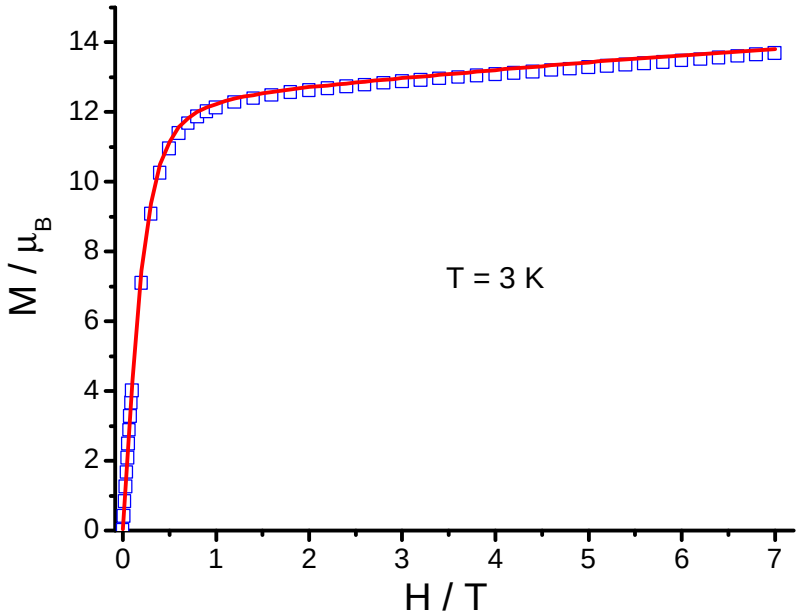

Figure S12. A comparison between experimental (square) and calculated (line) powder molar magnetization of the Dy_2Co_2 complex at 3K.

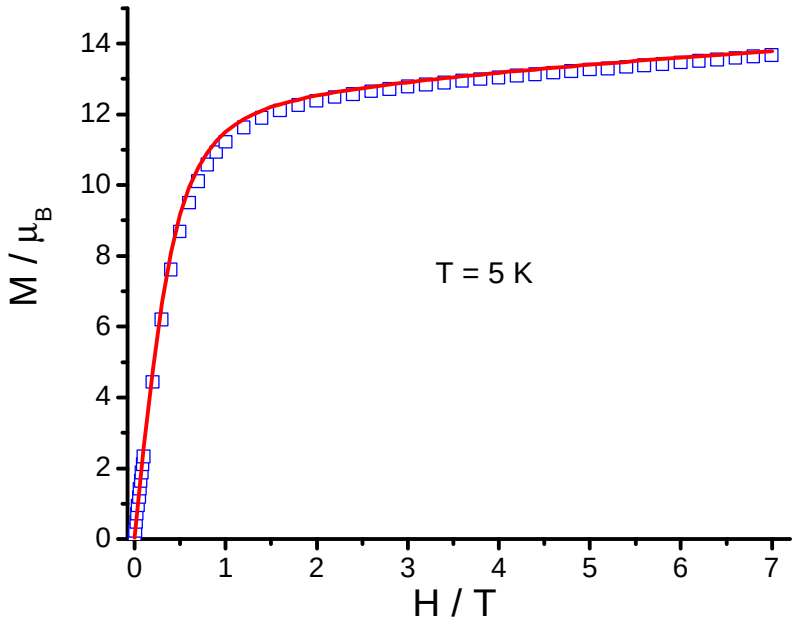

Figure S13 A comparison between experimental (square) and calculated (line) powder molar magnetization of the Dy_2Co_2 complex at 5K.

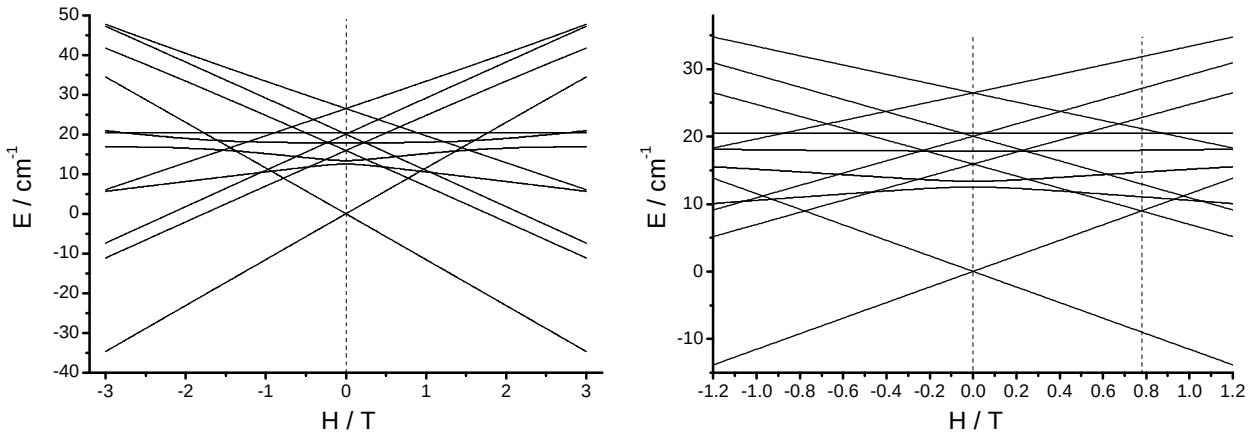

Figure S14. Evolution of the lowest energy levels in the applied magnetic field along the main magnetic axis of the Dy_2Co_2 complex.